

## Water-saturation estimation from seismic and rock-property trends

Zhengyun Zhou\*, Fred J. Hilterman, Haitao Ren, Center for Applied Geosciences and Energy, University of Houston, Mritunjay Kumar, Dept. of Geosciences, University of Houston

### Summary

The ability to estimate water saturation for a thin-bed reservoir from seismic is greatly enhanced if two rock-property transforms are employed. One transform linearly relates the wet normal-incident reflectivity [NI(wet)] to the hydrocarbon NI. The other transform relates the far-trace amplitude to NI for each saturation state. These transforms are derived from rock-property trends that are local to the prospect. With these two transforms and the AVO gathers at the prospect and at the down-dip water-equivalent reservoir, a test statistic can be developed that differentiates economic gas from fizz saturation. The methodology doesn't require a calibration well that ties the seismic unless the bed thickness is desired.

### Introduction

A reservoir is often called "fizz" when the gas percentage in the pore space is 25 percent or less. Normally, a small amount of gas in a reservoir lowers the P-wave velocity dramatically, and then as the gas saturation increases the primary velocity does not change significantly. The pore-fluid prediction becomes more difficult as reservoir properties such as porosity undergo slight changes. These possible reservoir scenarios make the prediction of fizz and gas from AVO problematic as is illustrated in Figure 1 (Hilterman, 2005).

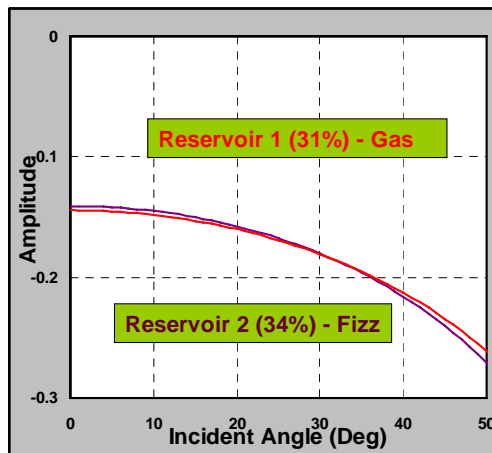


Figure 1: Similar AVO responses for fizz and gas reservoirs, reservoir 1 is at 6500 ft, reservoir 2 is at 4500 ft.

Obviously, with almost identical AVO curves in Figure 1, AVO inversion, even one with three terms, will not distinguish a fizz reservoir from gas. This paper will introduce rock-property transforms that assist in the discrimination of gas from fizz. The thickness of the reservoir can also be estimated.

### Seismic Field Example

In Figure 2, a gas reservoir is depicted along with a down-dip location where the sand reservoir is assumed to be wet. The migrated CDP gathers associated with the gas and wet locations are shown beneath the section. AVO synthetics generated by assuming thin-bed reservoirs are shown. The seismic wavelet was estimated by dynamically varying the frequency band and phase constant.

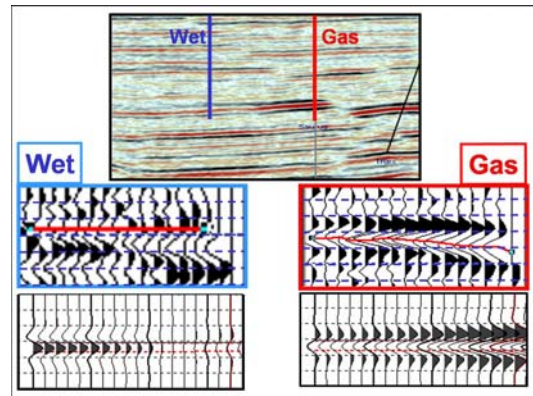


Figure 2: Seismic section (top) with migrated CDP gathers at gas reservoir and down-dip wet location (middle). Thin bed AVO synthetics were generated with interactive software where the rock properties were obtained from paper logs (bottom row).

In this area, it was anticipated that variations of the reservoir properties would change the hydrocarbon response and this is illustrated in Figure 3 where the velocity and density of the encasing shale properties were slightly increased. The synthetics based on the original rock properties are shown on the left for three saturations. With increased shale properties, a new lithology model is introduced and the synthetics for this new model are shown on the right. We find that the fizz-saturated reservoir for the new lithology model matches the gas-saturated synthetic for the known reservoir. This result is also depicted in Figure 1. However, the clue for discrimination

## Water saturation estimation

lies in the fact that the wet synthetics for the two models in Figure 3 are different.

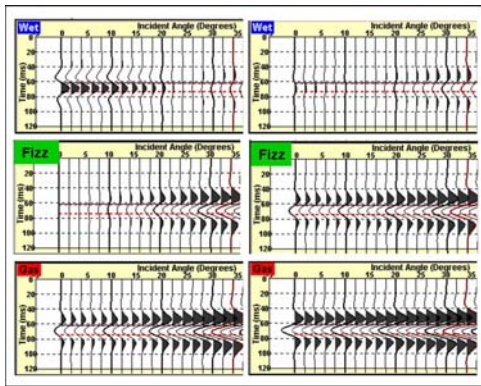


Figure 3: AVO synthetics on left are based on well model. On the right, the synthetics are based on the well properties with an increase in the shale velocity and density.

If the down-dip water-saturated AVO response is available, then it might be possible to distinguish fizz from gas. This possibility initiated a rock-property analysis to determine the expected AVO variations from the original well location.

### Rock-property observations and transforms

The rock-property variations in the area were estimated using histogram trend analyses generated by Geophysical Development Corporation (Hilterman, 2001). As an example, the histogram velocity trend shown in Figure 4 represents wet sand and was derived from 80 wells near the gas field. In all, velocity and density trends were available for wet sand and shale. Standard deviation values for velocity and density at the reservoir depth interval of 10000 ft were used to derive a suite of AVO curves representing expected variations in lithologies for the area.

Fluid properties were computed using the Batzle-Wang (1992) algorithms and the Greenberg-Castagna (1992) algorithms for estimating S-wave velocity for fluid substitution.

Seven models are used in this paper to illustrate the AVO deviation from the curves at the well location. They represent 1) original model; 2) increase shale properties; 3) decrease shale properties; 4) increase sand properties; 5) decrease sand properties; 6) increase both shale and sand properties; and 7) decrease both shale and sand properties. In all models, the increase or decrease was a one standard deviation of velocity and density (approximately 500 ft/s and .05 gm/cc).

Figure 5 compares the Zoeppritz curves for two of the deviation models. It is illustrated in the figure that the magnitude of the reflection coefficient curves vary

significantly when the rock-property deviations are introduced, but the difference NI(wet)-NI(gas) within a plot are relatively constant as depicted by the arrows. The same observation occurs for the other deviation models. Using all 7 models, quantifying local reflectivity transforms are presented in Figure 6. The coefficients in the two linear relationships (Equations 1 and 2) between NI(wet) and NI(gas) and between NI(wet) and NI(fizz) for 10000-ft depth are very similar to the results obtained from 239 deep-water reservoirs in the Gulf of Mexico (Hilterman and Liang, 2003)

$$NI(gas) = -0.08 + 1.12 NI(wet) \quad (1)$$

$$NI(fizz) = -0.05 + 1.06 NI(wet) \quad (2)$$

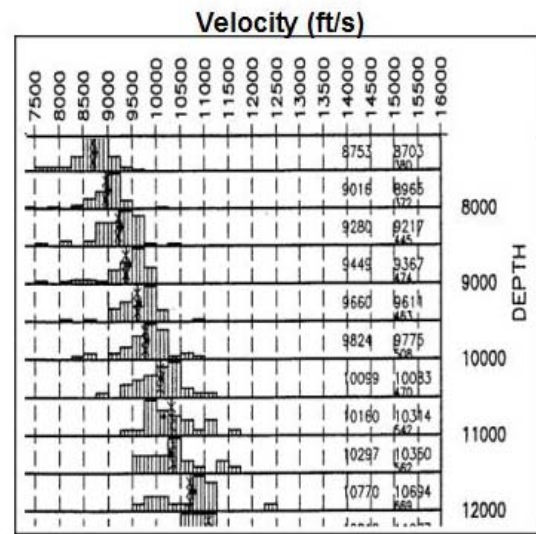


Figure 4: Regional trend of sand velocity generated from approximately 80 wells.

In each of the three AVO plots (Figure 5), the fizz and gas curves are approximately parallel. However, the slopes of the gas curves are proportional to the NI wet value. The more positive NI is, the larger the slope. The amplitude difference between the near and far traces is different for each model suggesting that changes in lithology can be related to the (far-near) amplitude value. In Figure 7, the far-trace amplitude, RC(30°), is expressed as a function of the near-trace amplitude, which we called the slope transform.

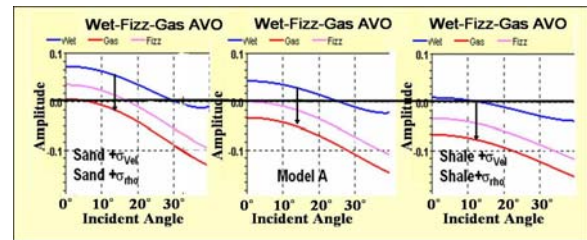


Figure 5: Zoeppritz curves for original and two deviation models.

## Water saturation estimation

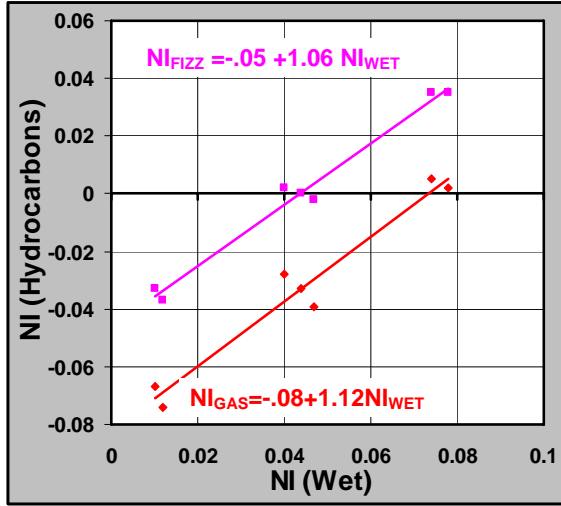


Figure 6: Quantifying local reflectivity transforms. (Pore Fluid Transforms)

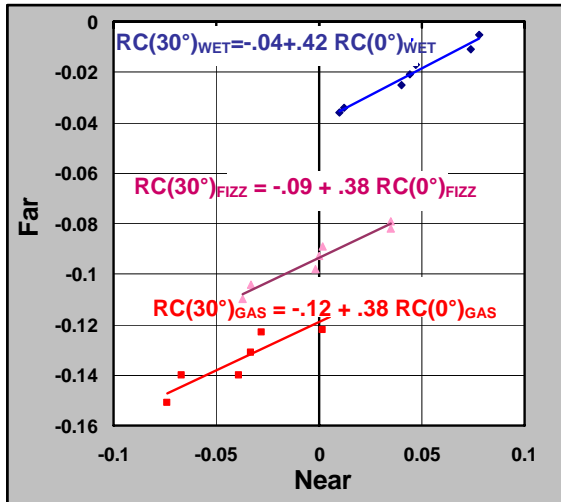


Figure 7: Linear relationships between  $RC(30^\circ)$  and  $RC(0^\circ)$  for wet, fizz and gas. (Slope Transforms)

The wet, gas and fizz saturations have different linear trends. Table 1 gives the coefficients for the three trends.

	Slope L1	Intercept L2
Wet	0.42	-0.04
Fizz	0.38	-0.09
Gas	0.38	-0.12

Table 1. Coefficients from Figure 7 for  $RC(30^\circ) = L1 * RC(0^\circ) + L2$ .

Equations (1) and (2) along with the trend equations in Figure 7 (or Table 1) represent the two rock-property transforms that will aid in discriminating fizz from gas. There are numerous methods of applying these two

transforms for pore-fluid discrimination. In fact, each of the authors had suggested different inversion styles.

### Seismic inversion for water saturation

Lin and Phair (1993) approximated the amplitude of a thin bed as

$$A(\theta) = k * \frac{4\pi b}{VT} * RC(\theta) * \cos(\theta) \quad (3)$$

where  $k$  is a constant,  $b$  is bed thickness,  $\theta$  is incident angle,  $A(\theta)$  is thin-bed seismic amplitude,  $RC(\theta)$  is reflection coefficient for upper boundary,  $V$  is interval velocity in the thin bed, and  $T$  is wavelet period. For the same seismic survey in a local area,  $k$  and  $T$  can be considered as constants. Now, an expression for  $k * (4\pi b/VT)$  is derived using the transforms.

From the transforms given in Table 1, the far-offset reflection coefficient can be expressed as

$$RC(30^\circ) = L1 * RC(0^\circ) + L2 \quad (4)$$

Equation (4) can be rewritten as

$$RC(30^\circ) - L1 * RC(0^\circ) = L2 \quad (5)$$

Starting with the seismic amplitude given by Equation (3),  $\theta$  is set to  $30^\circ$  and then the seismic amplitude at  $0^\circ$  is subtracted after being multiplied by  $L1$  to yield

$$\frac{A(30^\circ)}{\cos(30^\circ)} - L1 * A(0^\circ) \quad (6)$$

$$= k * \frac{4\pi b}{VT} * (RC(30^\circ) - L1 * RC(0^\circ))$$

Substituting Equation (5) into the right of Equation (6) yields

$$k * \frac{4\pi b}{VT} = \frac{A(30^\circ) - L1 * A(0^\circ)}{L2} \quad (7)$$

Combined Equations (3) and (7), we obtain  $RC(0^\circ)$  as

$$NI = RC(0^\circ) = \frac{A(0^\circ)}{k * \frac{4\pi b}{VT}} = \frac{A(0^\circ) * L2}{A(30^\circ) - L1 * A(0^\circ)} \quad (8)$$

The terms  $A(0^\circ)$  and  $A(30^\circ)$  represent the seismic amplitudes from the field CDP gathers. The values of  $L1$  and  $L2$  in Table 1 are used for different pore-fluid predictions. Thus, the  $NI$  value for the wet sand is estimated using the far and near trace amplitudes from the CDP gather down dip and the “Wet” coefficients in Table 1. The  $NI$  for the hydrocarbon-saturated reservoir is obtained from the CDP gather at the prospect and using the lower two rows in Table 1 to obtain both  $NI(\text{gas})$  or  $NI(\text{fizz})$ .

If the seismic modeling is quantitatively calibrated to the seismic data at the well location, then the constant value  $k$  in Equation (3) is known. Then at the down-dip location of the prospect,  $NI(\text{wet})$  can be found with Equation (8) and with an estimate of  $V$  for the wet sand, a prediction of the bed thickness  $b$  is possible with Equation (3).

## Water saturation estimation

### Estimation steps

Estimations of pore fluid are made in two steps (Figures 8a and 8b).

Step 1: Estimation in wet area.

Starting from the near and far amplitude maps, an estimate of the reflection coefficient in the brine-saturated down-dip area is made. The wet slope transform is used to get NI in wet area. With NI wet known in the down-dip areas, the pore-fluid transforms are applied to yield the NI of gas and NI of fizz in the down-dip areas. Since we have more confidence for the wet saturation NI, the maps of NI of gas and NI of fizz can be considered as standards.

Step 2: Estimation in hydrocarbon area

Both gas and fizz slope transforms are applied to the near and far amplitude maps, since the pore fluid in the hydrocarbon area is unknown. The gas test and fizz test of NI in the hydrocarbon area are compared with the standards. For the left reservoir, the gas test is closer to the standard than fizz test. And for the right reservoir, the fizz test is closer to the standard than gas test. So we can easily make the prediction that left reservoir is gas saturated and right reservoir is fizz.

### Discussion

The pore-fluid transforms in this area are very close to others measured in the Gulf of Mexico, indicating the pore-fluid transforms are quite robust. But the slope transforms are not as robust as pore-fluid transforms. They are depth and area dependent and should be generated for specific areas or depths. If a calibration well is provided for matching the seismic data, then the thickness at the prospect can be estimated. Obviously, noise in the CDP gather would decrease this discrimination technique that is already data processing sensitive.

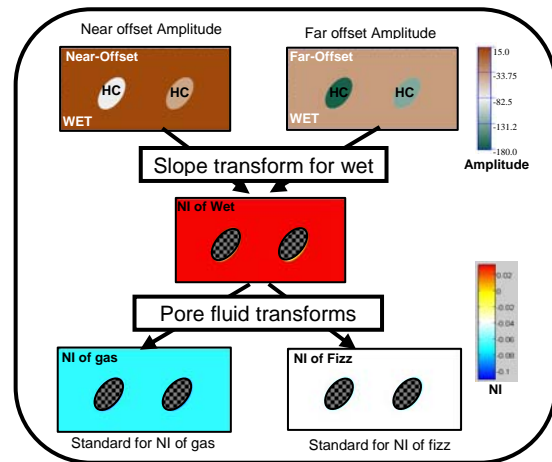
### Conclusions

From the analysis above, several conclusions are obtained:

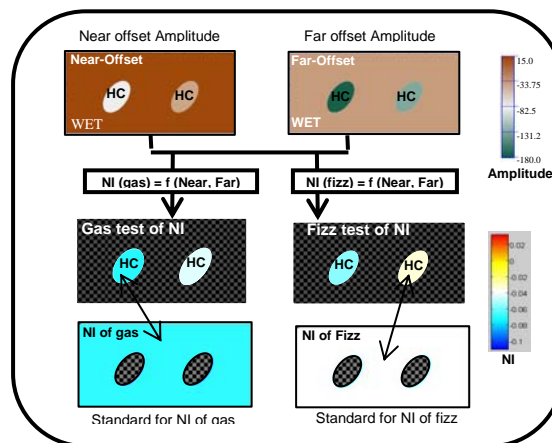
- 1) Fizz and gas reservoirs can have the same AVO responses, but down-dip water-saturated AVO responses can help to discriminate fizz from gas reservoirs.
- 2) NI of wet, gas and fizz saturations vary with changing rock properties. However, the values of  $(NI_{WET} - NI_{GAS})$  and of  $(NI_{WET} - NI_{FIZZ})$  remain fairly stable. In the *Pore-Fluid Transforms*, linear functions are used to predict  $NI_{GAS}$  and  $NI_{FIZZ}$  from  $NI_{WET}$ .
- 3) In our study area, the larger differences between the far- and near-offset reflection coefficients were associated with the more positive NI. This

observation relates to the lithologic differences across the reflection boundary. We have calibrated these relationships in our *Slope Transforms*.

- 4) With the Slope Transforms, the amplitudes of the processed seismic data can be converted into reflection coefficients. Once the NIs for the mapped area are predicted, the NI at the prospect area and at its down-dip wet equivalent combined with pore-fluid transforms are used to determine the water saturation.



(a) Step 1: Estimation in Wet Area



(b) Step 2: Estimation in hydrocarbon area

Figure 8: Estimation steps. (a) step 1, estimation in wet area; (b) step 2, estimation in hydrocarbon area.

### References

- Batzle, M., and Wang, Z., 1992, Seismic properties of fluids: *Geophysics*, 57, 1396-1408.
- Greenberg, M.L., and Castagna, J.P., 1992, Shear-wave velocity estimation in porous rocks: Theoretical

## Water saturation estimation

formulation, preliminary verification and applications:  
Geophys. Prosp., 40, 195-210

Hilterman, F.J., 2001, Seismic amplitude interpretation:  
Distinguished Instructor Series, No. 4, SEG and EAGE.

Hilterman, F.J., 2005, AVO Signatures: Gas to fizz  
variation = 31 to 34% porosity variation, Edger Forum,  
Univ. of Texas, Austin.

Hilterman, F.J. and Liang, L. , 2003, Linking rock-property  
trends and AVO equations to GOM deep-water reservoirs,  
73rd Ann. Internat. Mtg., Soc. Expl. Geophys., Expanded  
Abstracts, 211-214.

Lin. T.L. and Phair. R., 1993, AVO Tuning, 63rd Ann.  
Internat. Mtg., Soc. Expl. Geophys., Expanded Abstracts,  
727-730.

### Acknowledgments

We would like to thank Fairfield for permission to show the seismic data, Rocky Roden for assistance in preparing the seismic data through SMT AVOPAK, Geophysical Development Corporation for the rock-property trend curves in the prospect area and PSI for the modeling software TIPS. Portions of this work were prepared with the support of the U.S. Department of Energy under the Award No. DE-FC26-04NT15503. However, any opinions, findings, conclusions, or recommendations expressed herein are those of the authors and do not necessary reflect the views of DOE.